



Published in final edited form as:

Inorg Chem. 2008 March 17; 47(6): 2033–2038. doi:10.1021/ic7017083.

Mo^V Electron Paramagnetic Resonance of Sulfite Oxidase Revisited: The Low-pH Chloride Signal

Christian J. Doonan[†], Heather L. Wilson[‡], Brian Bennett[§], Roger C. Prince^{||}, K. V. Rajagopalan[‡], and Graham N. George^{*,†}

[†]Department of Geological Sciences, University of Saskatchewan, Saskatoon, Saskatchewan S7N 5E2, Canada

[‡]Department of Biochemistry, School of Medicine, Duke University, Durham, North Carolina 27710

[§]Department of Biophysics, Medical College of Wisconsin, 8701 Watertown Plank Road, Milwaukee, Wisconsin 53226

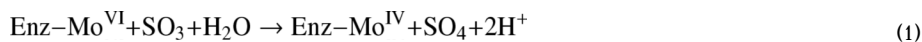
^{||}ExxonMobil Biomedical Sciences Inc., Annandale, New Jersey 08801

Abstract

Valuable information on the active sites of molybdenum enzymes has been provided by Mo^V electron paramagnetic resonance (EPR) spectroscopy. In recent years, multiple resonance techniques have been extensively used to examine details of the active-site structure, but basic continuous-wave (CW) EPR has not been re-evaluated in several decades. Here, we present a re-examination of the CW EPR spectroscopy of the sulfite oxidase low-pH chloride species and provide evidence for direct coordination of molybdenum by chloride.

Introduction

Sulfite oxidase (SO) is an oxo-transferase enzyme responsible for the physiologically vital oxidation of sulfite to sulfate.¹ Residing in the mitochondrial inner-membrane space, the enzyme is dimeric with a subunit mass of about 52 000. Each monomer contains molybdenum associated with a single pterin cofactor, and a cytochrome *b*₅-type heme. The two-electron oxidation of sulfite to sulfate is known to occur at the molybdenum site, which is concomitantly reduced from Mo^{VI} to Mo^{IV}.



The catalytic cycle is completed with reoxidation of the molybdenum first to Mo^V, and then to Mo^{VI}, by intramolecular electron transfer to the cytochrome *b*₅ site, with cytochrome *c* serving as the external electron acceptor.^{2,3}

With the exception of nitrogenase,⁴ all molybdenum enzymes described to date contain a novel pyranopterin-dithiolene cofactor (known as molybdopterin) in which the molybdenum is coordinated by the dithiolene moiety.^{5,6} In SO, the molybdenum atom is coordinated by one

dithiolene, with two terminal oxygen atoms and one additional sulfur ligand from a cysteine (Cys²⁰⁷ in human SO).⁷ As one of the most intensively studied molybdenum enzymes, SO can be regarded as the prototypical member of the family of molybdenum enzymes possessing a dioxo molybdenum structural motif when in the fully oxidized Mo^{VI} form.⁸

One of the major spectroscopic techniques that has provided information on the active site is Mo^V electron paramagnetic resonance (EPR). Recently, efforts have been focused on studying SO using advanced pulsed EPR techniques, such as electron–nuclear double resonance (ENDOR) and electron-spin envelope echo modulation (ESEEM),⁹ but the conventional continuous-wave (CW) EPR has not been re-evaluated in nearly two decades. In this work, we revisit the Mo^V EPR of one of the major signals from this important enzyme,^{11–13} and using the stable magnetic isotopes ³⁵Cl and ³⁷Cl, in conjunction with difference EPR spectroscopy, and analogous complexes with other halides, we present new evidence for halide molybdenum coordination of the Mo^V low-pH species.

Materials and Methods

CW EPR spectroscopy

X-band EPR spectra were recorded on Varian E109 or Bruker EMX spectrometers. S-band spectra were recorded on a custom-built loop-gap resonator¹⁴ equipped with a 2–4 GHz bridge (Medical Advances, Milwaukee, WI) at the National Biomedical EPR Center. Data acquisition, analysis, and EPR computer simulations were performed as previously described,^{14–16} except that a modulation amplitude of 0.05 mT was used. For the Bruker EMX system, 4096 field points across the scan were taken, whereas for the Varian spectrometers, 1024 field points were used.

Samples

Purified recombinant human sulfite oxidase was obtained as previously described.¹⁷ Mo^V EPR signals were generated by the addition of 1 mM (final) sodium sulfite solution to concentrated enzyme (approximately 0.25 mM Mo) before freezing in quartz sample tubes of 3 mm internal diameter. A mixed buffer system was used, consisting of 50 mM bis-tris-propane and 50 mM MES. Reagents were obtained from Sigma-Aldrich Chemical Co. and were of the best quality available. Isotopically enriched Na³⁵Cl and Na³⁷Cl were obtained from Oak Ridge National Laboratories at isotopic enrichments of 99.9 and 98.2 atom %, respectively.

Molecular Modeling

Density functional theory (DFT) molecular modeling used the program Dmol3 Materials Studio, version 3.2.^{18,19} We expected bond-length accuracies of around 0.05 Å, and good estimates of energetic trends between postulated molecular entities. The Becke exchange²⁰ and Perdew correlation functionals²¹ were used to calculate both the potential during the self-consistent field procedure and the energy. Double numerical basis sets included polarization functions for all atoms. Calculations were spin-unrestricted, and all electron relativistic core potentials were used. No symmetry constraints were applied, and optimized geometries used energy tolerances of 2.0×10^{-5} Hartree.

Results and Discussion

Mo^V Electron Paramagnetic Resonance Spectroscopy

Figure 1 compares the high-pH signal and low-pH Mo^V EPR signals of human SO. Both have an exchangeable strongly coupled proton thought to originate from Mo–OH coordination, but a well-resolved splitting is only seen for the low-pH signal. The splitting is not directly observed for the high-pH signal, but its presence is betrayed by formally forbidden $\Delta m_I = \pm 1$ satellites

separated by the proton frequency (the so-called proton spin-flip lines).^{16,22} Two different explanations have been suggested for the lack of observed proton hyperfine splittings in the high-pH signal; both assume a proton coordinated as Mo–OH with a small isotropic coupling and postulate different reasons why the anisotropic splitting is not directly observed. The first hypothesizes that the anisotropic proton hyperfine tensor and the g tensor are oriented close to the so-called trimagic angle, resulting in essentially no anisotropic splittings at each of the principal g values (g_x , g_y , and g_z), whereas the $\Delta m_I = \pm 1$ will be at maximal intensity, and thus readily observed.¹⁶ Computer simulations showed that this suggestion could account for the powder line shape of the high-pH signal.^{16,23} The second suggestion followed confirmation of the presence of proton hyperfine splitting by pulsed EPR spectroscopy²⁴ and conjectured that rotational averaging about the Mo–O bond caused essentially zero anisotropic splittings at each g_x , g_y , and g_z .²⁴ Which of these two suggestions more accurately explains the lack of proton splitting in the SO high-pH EPR signal remains uncertain. Previous work has shown that the addition of chloride promotes the conversion of the high-pH species to the low-pH species.¹³ Moreover, Bray and co-workers found that increasing the chloride concentration by a factor of 10 shifted the pK_a of the interconversion between high- and low-pH signal-giving species by one pH unit.¹³ In addition, they reported that the low-pH EPR signals were identical in the absence and presence of chloride and attributed this to trace amounts of contaminating chloride in their “chloride-free” buffers.²⁵ Figure 1b and c compare the low-pH spectra obtained in the presence and in the rigorous absence of added chloride. The signal obtained in the presence of chloride is essentially identical to that obtained by Bray et al., but the spectrum in the absence of chloride is clearly different, possessing slightly different g values and much narrower line widths (Table 1).²⁶ We will use this EPR signal-giving species as the low-pH halide-free species. The observed pK relating the high-pH and low-pH EPR signal-giving species shifts from 8.1 in the absence of chloride to 6.8 in the presence of 0.1 M chloride (Figure 2), which approximately corresponds to the lowest pK measured by Bray and co-workers¹³ and might suggest a difference in structure at the active site in the presence and absence of chloride.

The broad line widths of the low-pH chloride signal have previously been attributed to unresolved hyperfine interaction with $I = 3/2$ ^{35}Cl and ^{37}Cl nuclei.^{13,28} However, this idea has fallen out of favor because chlorine hyperfine coupling has remained undetected by ENDOR. Thus, the structures currently postulated for the low-pH signal are five-coordinate species, as shown in Figure 3.⁹ Our finding of a sharper line width for the low-pH halide-free signal supports the original hypothesis of unresolved chlorine hyperfine coupling and encouraged us to perform further experiments using the stable magnetic isotopes ^{35}Cl and ^{37}Cl . Figure 4 shows the low-pH Cl^- spectra at X- and S-band microwave frequencies obtained with ^{35}Cl - and ^{37}Cl -enriched sodium chloride. These two isotopes both have $I = 3/2$, but ^{35}Cl has a slightly larger nuclear g value than ^{37}Cl ($g_N = 0.548$ and 0.456 , respectively), and proportionally larger hyperfine couplings are expected. Subtle but fully reproducible differences between ^{35}Cl and ^{37}Cl are observed, which are best visualized by examining the difference spectra (Figure 4). The EPR difference spectra simulations of Figure 4 were computed using the line widths of the low-pH halide-free signal (e.g., Figure 1c), and simulating the broader lines of the ^{35}Cl spectrum using unresolved hyperfine coupling to an $I = 3/2$ nucleus. Some effects due to nuclear electric quadrupole coupling to the chlorine nuclei are expected to be present. The nuclear electric quadrupole moments of the two nuclei are quite small, at only -0.079 and -0.062 b for ^{35}Cl and ^{37}Cl , respectively, but the nuclear electric quadrupole coupling will gain in magnitude due to the significant electric field gradient expected for coordinated chloride. Unless the quadrupole coupling is very large,²⁹ quadrupole effects are usually manifested as additional transitions approximately within the envelope of the hyperfine splitting.^{30,31} Furthermore, no obvious quadrupole effects are observed in the EPR spectra of other transition metal ions exhibiting chlorine hyperfine coupling.^{32,33} As we observe only a broadening, our estimates of hyperfine couplings will necessarily be approximate, and quadrupole effects can

be safely neglected in our current simulations without substantially changing our conclusions. Difference simulations were generated by subtracting the normalized ^{37}Cl simulation from the normalized ^{35}Cl simulation, with the former being obtained by reducing the chlorine couplings by the ratio of nuclear g values (0.83).³⁴ Our simulations of the observed broadenings yielded an approximate hyperfine coupling (^{35}Cl) $A_{(x,y,z)} = 3.9, 4.9, \text{ and } 3.0 \text{ MHz}$.³⁵ The similarity of the experimental and simulated spectra in Figure 4 provides strong evidence that hyperfine coupling to chlorine in the range of 3–5 MHz is present in the low-pH chloride species. The observation of similar line broadening of the EPR spectra at the two microwave frequencies effectively eliminates g strain as the primary source of broadening in the low-pH chloride species.³⁶ We note that a complete quantitative determination of this hyperfine coupling is not possible with X- and S-band EPR. Hyperfine coupling arises from such mechanisms as electron delocalization, exchange terms such as spin polarization, and direct dipole coupling. Sulfite oxidase contains an arginine-rich pocket $\sim 5 \text{ \AA}$ from Mo, and Cl^- has been observed crystallographically in this pocket in the structure of a mutant sulfite oxidase.³⁷ The dipole coupling at this distance will be only 0.1 MHz, and at such large distances, other mechanisms of coupling are very unlikely. We can thus effectively exclude the 5 \AA pocket as the origin of the observed hyperfine coupling. Typical Mo–Cl bond lengths for high-valent Mo species range from 2.38 to 2.65 \AA (cis and trans to an Mo=O ligation, respectively).³⁸ Simple dipole hyperfine calculations using these bond lengths yield a maximum ^{35}Cl dipole coupling contribution of 1.2 and 0.8 MHz, respectively, and additional mechanisms will increase these values (vide supra). Thus, the chlorine hyperfine broadening of the Mo^{V} EPR signal that we observe provides strong evidence for direct coordination of chloride to Mo. Furthermore, the similarity in spin Hamiltonian parameters for the low-pH Cl^- and low-pH halide-free signals (Figure 1) cannot be reconciled with an equatorial coordination of the anion, as this would be expected to influence the g values through bonding interaction with the magnetic $\text{Mo } 4d_{xy}$ orbital. Thus, we postulate that the low-pH Cl^- species is six-coordinate with the chloride coordinated trans to the Mo=O ligand. In addition, we hypothesize that the structure of the high-pH species is analogous to the five-coordinate Mo site established from protein crystallography and extended X-ray absorption fine structure (EXAFS) spectroscopy (Figure 3). The low-pH signal prepared in the absence of halide (low-pH halide-free, Figure 1) has very similar g values and ^1H hyperfine couplings to the low-pH and must have a similar active-site structure, possibly with sulfate or sulfite occupying the axial position instead of chloride. This description of the active site is consistent with the observed shift to higher g values for the low-pH Cl^- species as the coordination change will effectively raise the donor orbitals of the dithiolene ligand into the plane of the half-occupied ground-state $\text{Mo } 4d_{xy}$, thus facilitating spin-delocalization onto the dithiolene sulfur ligands through spin-orbit coupling.

In agreement with earlier work, we were unable to detect any X-band ENDOR signals attributable to ^{35}Cl and ^{37}Cl (see the Supporting Information). However, weakly magnetic quadrupolar nuclei such as ^{35}Cl and ^{37}Cl are often difficult to detect by ENDOR unless high microwave frequencies are used to increase the relative size of the nuclear Zeeman term.³⁹ Bray and co-workers also reported a minor species attributed to a low-pH fluoride complex of sulfite oxidase with resolved ^{19}F coupling. This would be expected because the ^{19}F coupling will be inherently larger than the $^{35,37}\text{Cl}$ coupling by approximately a factor of 10. However, we were unable to reproduce their results, possibly because of very subtle differences between the chicken enzyme used by Bray and the human enzyme which is the subject of the present study. Furthermore, we note that Bray's fluoride spectrum was a minor component and needed to be generated by taking multiple difference spectra. This technique is somewhat prone to artifacts, and whether Bray actually detected a bona fide fluoride species is debatable. Moreover, fluoride is not expected to be a good axial ligand, trans to the Mo=O group, thus our inability to detect a well-defined fluoride complex is not surprising. Mo^{V} complexes of bromide and iodide are known,^{40,41} and these anions should also give larger hyperfine couplings than chloride, and the effects of these anions on the EPR spectrum of SO are thus

of relevance to the low-pH chloride signal. Bromine has two naturally abundant stable magnetic isotopes ^{79}Br and ^{81}Br (50.5 and 49.5% natural abundance, respectively), both with $I = 3/2$ and with similar nuclear g values (1.404 and 1.513, respectively). Iodine has a single stable magnetic isotope ^{127}I with $I = 5/2$ and a nuclear g value of 1.872. If all other factors are equal, both anisotropic and isotropic hyperfine couplings to bromine and iodine are expected to be similar, and about a factor of approximately 4.5 larger than those to chlorine. Figure 5 compares the signals obtained in the presence of bromide and iodide with those from chloride. Clearly resolved hyperfine splittings can be seen for both bromide and iodide signals. The signals also have well-resolved proton hyperfine splittings, which were demonstrated by development of the signals in $^2\text{H}_2\text{O}$ (not illustrated). Computer simulation was used to quantify the couplings to halide nuclei. We note that bromine and iodine nuclei have significant quadrupole moments (+0.310 and +0.260 b for ^{79}Br and ^{81}Br , respectively, and -0.790 b for ^{127}I). Because of this, we included nuclear electric quadrupole coupling in our simulations. As previously discussed,⁴² the number of parameters included in simulations such as these is large, and unambiguous determination of the spin Hamiltonian parameters requires spectroscopy at higher microwave frequencies. Nevertheless, the observation that strong hyperfine coupling is present to both bromine and iodine is unambiguous and provides very strong support for the hypothesis of the direct coordination of a halide ligand to Mo in the low-pH halide EPR signal-giving species.

This possibility was further tested using density functional calculations, and Figure 6 shows the results of energy minimizations including three of the active-site amino acids (tyrosine 343, arginine 160, and cysteine 207). The α carbons of the amino acids and the pyran ring carbons were constrained to their crystallographic positions, as were the vectors described by the α and β carbons. The results of energy minimizations were found to be very sensitive to the exact starting coordinates; for example, changing the orientation of the $-\text{OH}$ group of tyrosine 343 was found to change the result of energy minimization between five-coordinate and six-coordinate, and thus our DFT calculations are of little use as a predictive tool for the active site structure. Nevertheless, the finding of well-defined Mo^{V} structures with and without Cl^- bound to Mo indicates that our hypothesis of chloride binding to the low-pH species is at least chemically reasonable. Moreover, when tyrosine 343 was omitted from the calculations, chloride typically dissociated from Mo during the energy minimization, suggesting that this amino acid is very important in stabilizing the complex. Figure 6 indicates two different possible Mo–OH orientations, one where the Mo–OH proton is hydrogen-bonded to the tyrosine oxygen (Figure 6a), corresponding to the high-pH species, and the other where the proton of the tyrosine $-\text{OH}$ group is hydrogen-bonded to the oxygen of the Mo–OH (Figure 6b), corresponding to the low-pH/chloride species. Conformational differences such as these will significantly affect the orientation of the anisotropic proton hyperfine coupling and may explain the different proton hyperfine splittings observed for the high-pH and low-pH chloride Mo^{V} EPR signals; although, as we have discussed above, the exact nature of the proton coupling to the high-pH species is still controversial.

Finally, our results are fully consistent with our earlier EXAFS studies of chicken sulfite oxidase which suggested an increase in Mo–S/Cl ligation with reduced conditions of low-pH Cl^- formation, relative to those of high-pH formation.^{43,44} Furthermore, our recent finding that a sulfite oxidase clinical mutant (arginine 160 \rightarrow glutamine) has a six-coordinate active site in the Mo^{VI} state (and in some Mo^{V} forms)⁴⁵ further supports our hypothesis for a six-coordinate structure for the low-pH chloride species. The apparent conformational flexibility of the reduced active site suggested by our new findings may have important implications for the catalytic mechanism. The availability of chloride in the mitochondrial inner-membrane space raises questions about the possibility of *in vivo* chloride coordination of Mo. Furthermore, the fact that the active site of the native enzyme can apparently adopt both six-coordinate and five-coordinate geometries may be important in the catalytic mechanism, which may involve the binding of anions such as sulfite directly to Mo.

Supplementary Material

Refer to Web version on PubMed Central for supplementary material.

Acknowledgments

Work at the University of Saskatchewan was supported by a Canada Research Chair award (G.N.G.), the University of Saskatchewan, the Province of Saskatchewan, the Natural Sciences and Engineering Research Council (Award #283315), the Canadian Institute for Health Research, and the Canada Foundation for Innovation (Award #201742). Work at Duke University was supported by NIH grant GM 00091. The National Biomedical EPR Center is supported by NIH NIBIB EB001980.

References

- (1). McLeod RM, Farkas W, Fridovitch I, Handler P. J. Biol. Chem 1961;236:1841–1852. [PubMed: 13764978]
- (2). Cohen HL, Betcher-Lange S, Kessler DL, Rajagopalan KV. J. Biol. Chem 1972;247:7759–7766. [PubMed: 4344230]
- (3). Johnson JL, Rajagopalan KV. J. Biol. Chem 1977;252:2017–2025. [PubMed: 14956]
- (4). Rees DC, Tezcan A, Haynes CA, Walton MY, Andrade S, Einsle O, Howard JB. Philos. Trans. R. Soc. London, Ser. A 2005;363:971–984.
- (5). Elliot SJ, McElhane AE, Feng C, Enemark JH, Armstrong FJ. J. Am. Chem. Soc 2002;124:11612–11613. [PubMed: 12296723]
- (6)(a). Rajagopalan KV. Adv. Enzymol. Relat. Areas Mol. Biol 1991;64:215–290. [PubMed: 2053467]
(b) Rajagopalan KV, Johnson JL. J. Biol. Chem 1992;267:10199–10202. [PubMed: 1587808]
- (7). Kisker C, Schindelin H, Pacheco A, Wehbi WA, Garrett RM, Rajagopalan KV, Enemark JH, Rees DC. Cell 1997;91:1–20. [PubMed: 9335327]
- (8). Hille R. Chem. Rev 1996;96:2757–2816. [PubMed: 11848841]
- (9). Enemark JH, Astashkin AV, Raitsimring AM. J. Chem. Soc., Dalton Trans 2006:3501–3514.
- (10). The portion of work describing the coupling of ^{35}Cl and ^{37}Cl was originally submitted as a communication in August 2006. Our data thus predate later suggestions of chlorine coupling by others.
- (11). Lamy MT, Gutteridge S, Bray RC. Biochem. J 1980;185:397–403. [PubMed: 6249254]
- (12). Cramer SP, Johnson JL, Rajagopalan KV, Sorrell TN. Biochem. Biophys. Res. Commun 1979;91:434–439. [PubMed: 229850]
- (13). Bray RC, Gutteridge S, Lamy MT, Wilkinson T. Biochem. J 1983;211:227–236. [PubMed: 6307274]
- (14). Frocisz W, Hyde JS. J. Magn. Reson 1982;47:515–521.
- (15). George GN, Prince RC, Kipke CA, Sunde RA, Enemark JE. Biochem. J 1988;256:307–309. [PubMed: 2851985]
- (16). George GN. J. Magn. Reson 1985;64:384–394.
- (17). Temple CA, Graf TN, Rajagopalan KV. Arch. Biochem. Biophys 2000;383:281–287. [PubMed: 11185564]
- (18). Delley B. J. Chem. Phys 1990;92:508–517.
- (19). Delley B. J. Chem. Phys 2000;113:7756–7764.
- (20). Becke AD. J. Chem. Phys 1988;88:2547–2553.
- (21). Perdew JP, Wang Y. Phys. Rev. B: Condens. Matter Mater. Phys 1992;45:13244–13249.
- (22). Proton spin-flip lines are formally forbidden $\Delta m_I = \pm 1$ transitions that are often observed in the EPR of free-radical systems when weakly coupled protons are present. Both proton spin-flip and double spin-flip lines (the latter involving two coupled protons) were the subject of an earlier study on the Mo^{V} EPR of molybdenum enzymes.¹⁶ The sulfite oxidase high-pH signal was alone among all the signals studied in having a strongly coupled exchangeable proton with no observed splittings, the presence of which was betrayed by the spin-flip lines.
- (23). Doonan CJ, Kappler U, George GN. Inorg. Chem 2006;45:7488–7492. [PubMed: 16933953]

- (24). Astashkin AV, Mader ML, Pacheco A, Enemark JH, Raitisimring AM. *J. Am. Chem. Soc* 2000;122:5294–5302.
- (25). Chloride is rather difficult to eliminate from solution, as there are many sources that are not usually accounted for, such as the KCl contained within the electrode used to measure the pH of samples, some of which will diffuse into the solution. Bray and co-workers¹³ estimated a contaminating level of chloride of 0.1 mM, and we expect our levels to be similar.
- (26). The lower concentrations of enzyme available to Bray et al. meant that these workers used a comparatively large modulation amplitude of 0.25 mT, which would have broadened the chloride-free low-pH signal so that it looked very similar to the signal obtained in the presence of chloride.
- (27). We note in passing that developing the signals in ²H₂O causes a broadening of the Mo^V EPR signal due to unresolved ²H hyperfine splitting, which makes the difference in broadening caused by ³⁵Cl and ³⁷Cl much harder to discern.
- (28). We note that the high ionic strengths caused by the use of high chloride concentrations might induce strain distributions in spin Hamiltonian parameters (e.g., *g*-strain), resulting in the observed broadening. This is not likely because low-pH Cl⁻ spectra developed at low pH using low concentrations of chloride (2 mM) are identical within the noise to those obtained at higher (100 mM) or very high (1 M) chloride concentrations.
- (29). George GN, Bray RC. *Biochemistry* 1983;22:5443–5432.
- (30). George GN, Bray RC. *Biochemistry* 1988;27:3603–3609. [PubMed: 2841971]
- (31). Connelly NG, Emslie DJH, Klansinsirikul P, Rieger PH. *J. Phys. Chem. A* 2002;106:12214–12220.
- (32). Petersen JL, Egan JW Jr. *Inorg. Chem* 1983;22:3571–3575.
- (33). Kon H, Sharpless NE. *J. Chem. Phys* 1965;43:1081–1082.
- (34). Simulations and spectra were in all cases normalized to their maximum amplitude. An alternative might be to normalize to the integrated intensity, but for experimental spectra, this is subject to an approximately 10% error (depending on a number of factors, such as baseline noise etc.), and because of this, normalizing to the amplitude is preferred.
- (35). We note that we estimate the sign of the hyperfine couplings.
- (36). Hagen WR. *J. Magn. Reson* 1981;44:447–469.
- (37). Karakas E, Wilson HL, Graf TN, Xiang S, Jaramillo-Busquets S, Rajagopalan KV, Kisker C. J. *Biol. Chem* 2005;280:33506–33515. [PubMed: 16048997]
- (38). This value is an average of all high-valent Mo entries with Mo–Cl coordination in the Cambridge Structure Database: Allen FH, Kennard O, Watson DG. *Struct. Correl* 1994;1:71–110.
- (39). We note that ESEEM features attributable to chloride have recently been reported: Astashkin AV, Klein EL, Enemark JH. *J. Inorg. Biochem* 2007;101:1623–1629. [PubMed: 17644181]
- (40). Cotton FA, Luck RL, Miertschin CS. *Inorg. Chem* 1991;30:548–553.
- (41). Baird DM, Rheingold AL, Croll SD, DiCenso AT. *Inorg. Chem* 1986;25:3458–3461.
- (42). George GN, Garrett RM, Graf T, Prince RC, Rajagopalan KV. *J. Am. Chem. Soc* 1998;120:4522–4523.
- (43). George GN, Kipke CA, Prince RC, Sunde RA, Enemark JH, Cramer SP. *Biochemistry* 1989;28:5075–5080. [PubMed: 2548601]
- (44). Note that chlorine and sulfur backscatterers cannot be distinguished by EXAFS; thus, coordination of a chloride would appear as an effective increase in the Mo–S coordination.
- (45). Doonan CJ, Wilson HL, Rajagopalan KV, Garrett RM, Bennett B, Prince RC, George GN. *J. Am. Chem. Soc* 2007;129:9421–9428. [PubMed: 17608478]

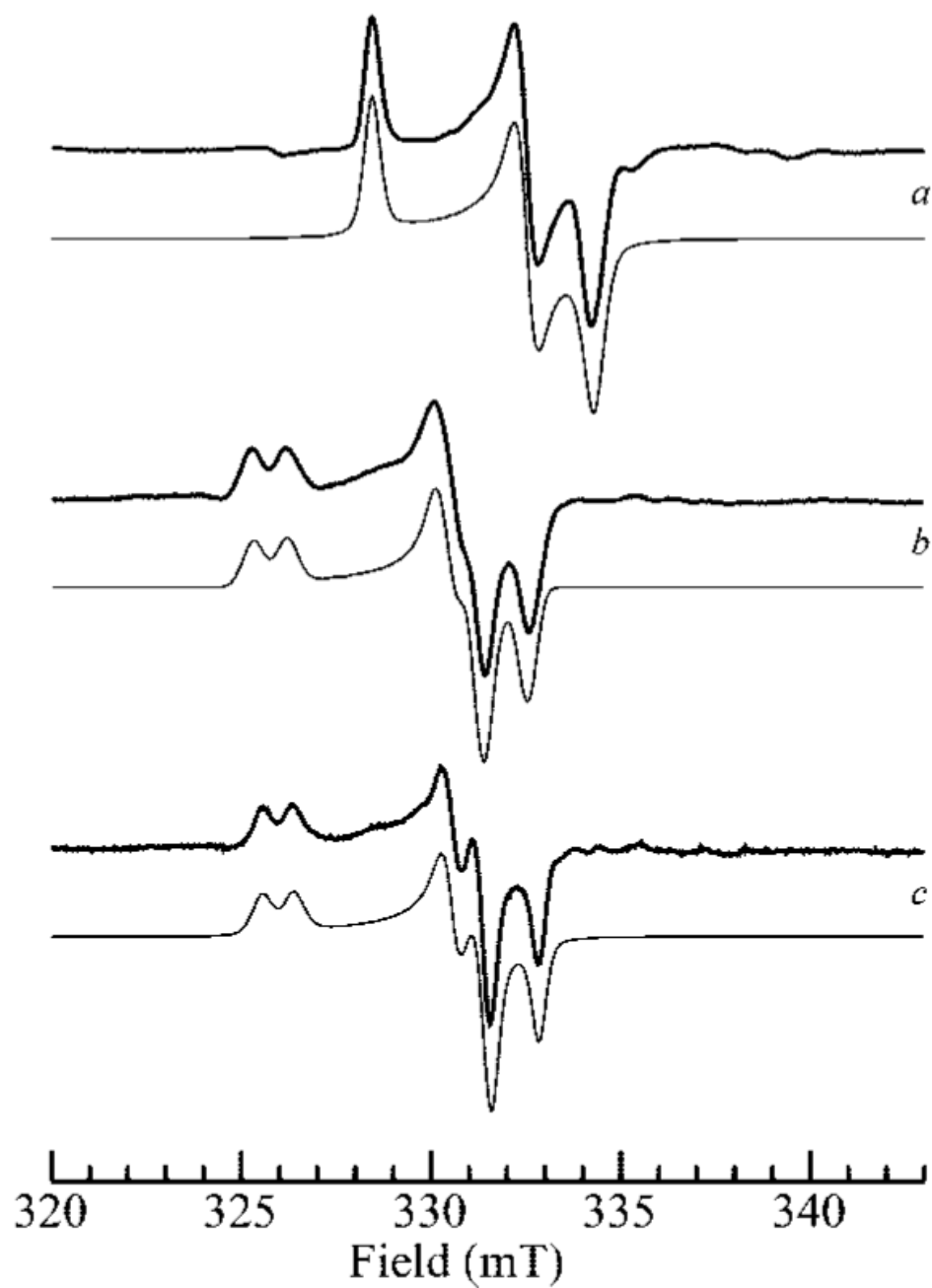


Figure 1. Effects of pH and chloride on Mo^V EPR spectra of human sulfite oxidase. Part a shows the high-pH species at pH 9.0 in ²H₂O; parts b and c show the low-pH species (pH 6.0) in the presence of 0.1 M Cl⁻ (b) and in the absence of chloride (c). Traces shown as bold lines are experimental data, and traces shown as light lines are computer simulations.

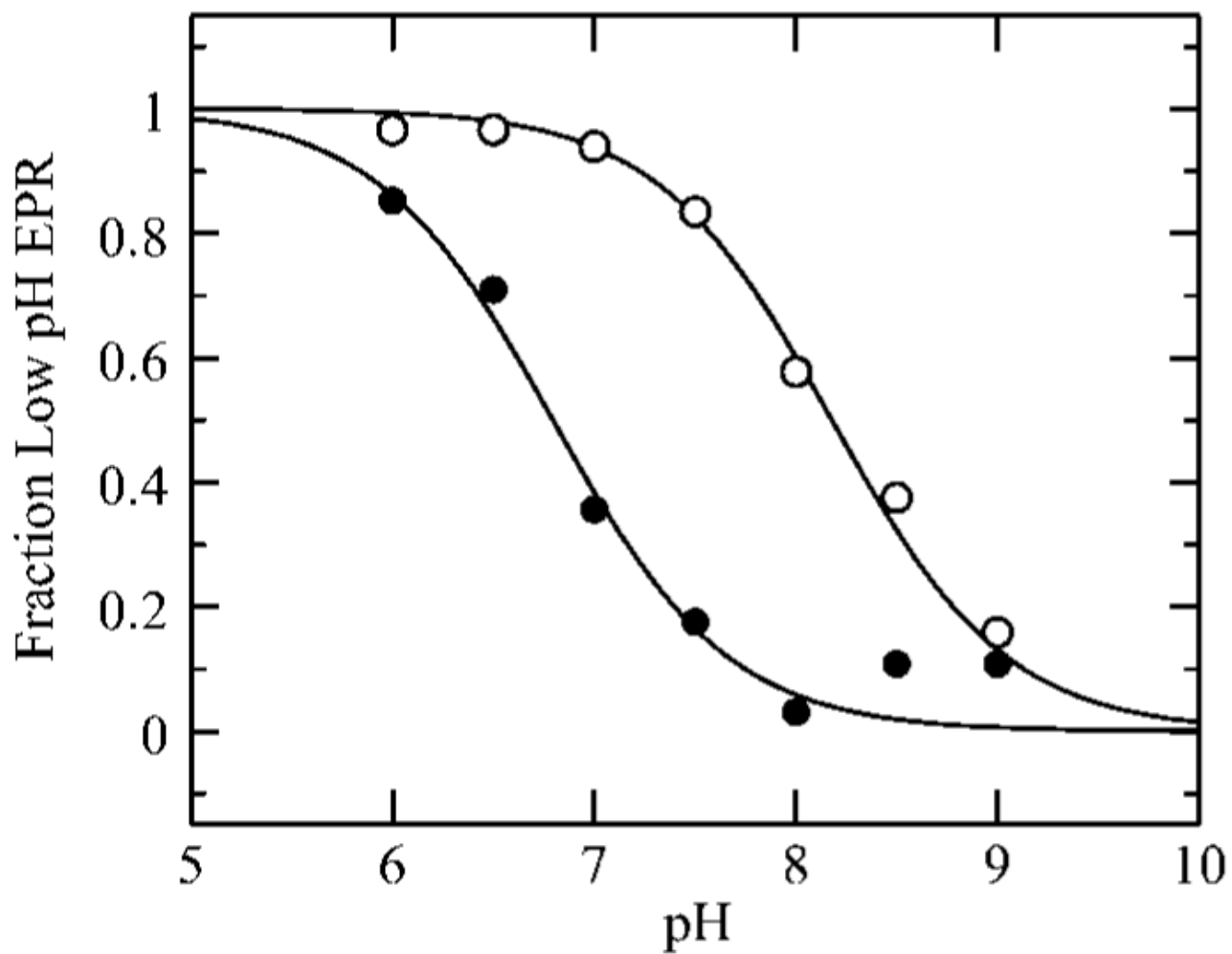


Figure 2. The pH dependency of the high-pH to low-pH conversion in the stringent absence of chloride (○) and in the presence of 0.1 M NaCl (●). The pK_a values determined from these data are 8.1 and 6.8, for no chloride and for 0.1 M NaCl, respectively.

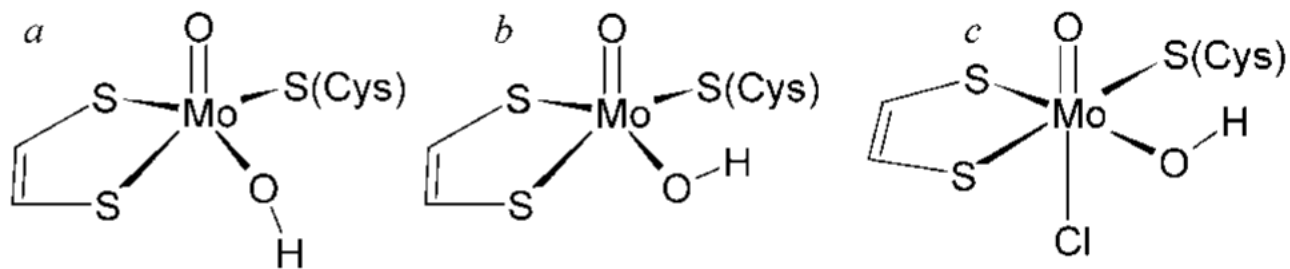


Figure 3. Previously postulated structures for the high-pH (a) and low-pH (b and c) signal-giving species.

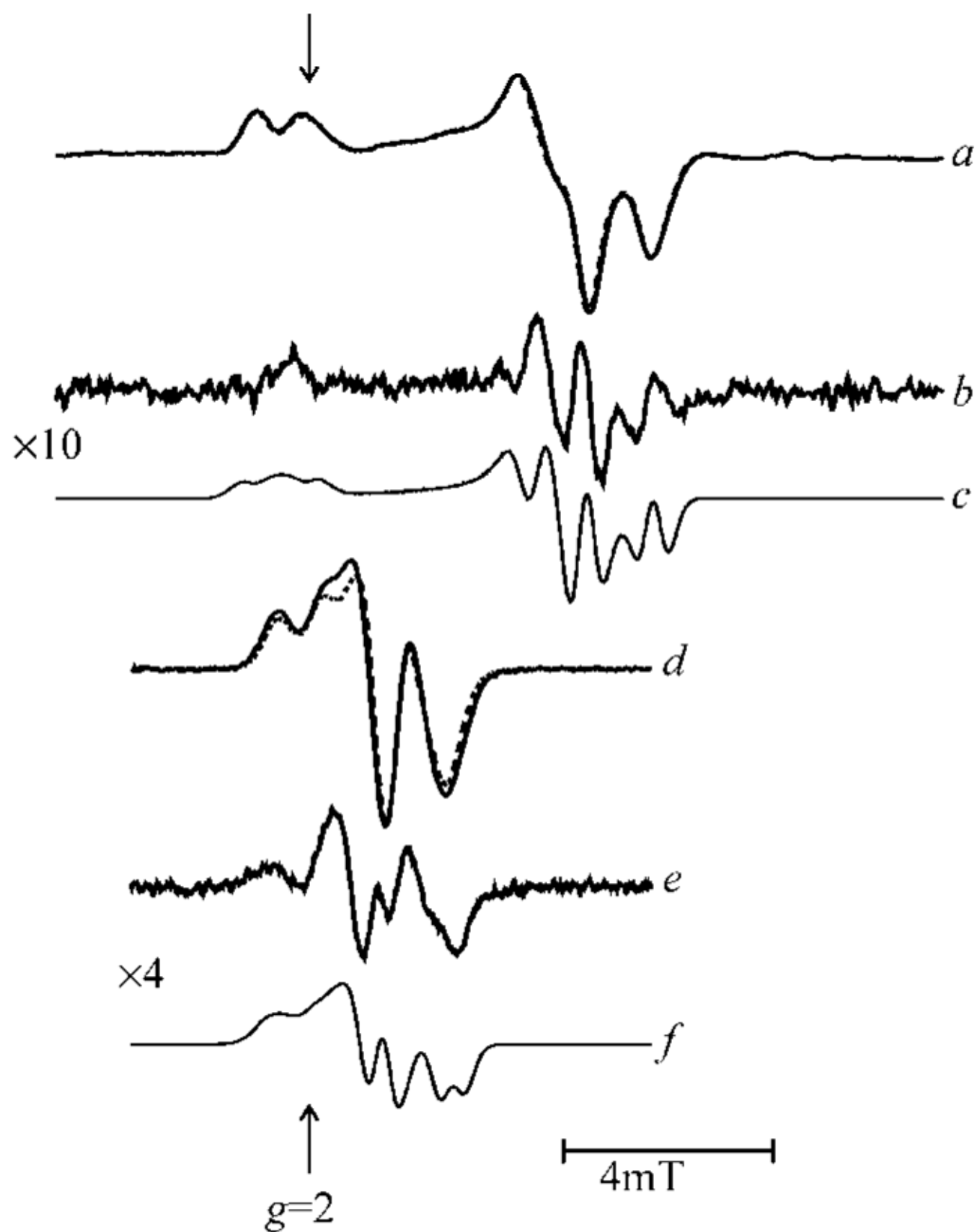


Figure 4. ^{35}Cl and ^{37}Cl isotope effects on the low-pH chloride EPR signal at X-band and at S-band microwave frequencies. Traces a and d compare signals from ^{35}Cl (solid line) and ^{37}Cl (broken line) at the X- and S-band, respectively; traces b and e show the corresponding difference spectra, and c and f the corresponding simulations.

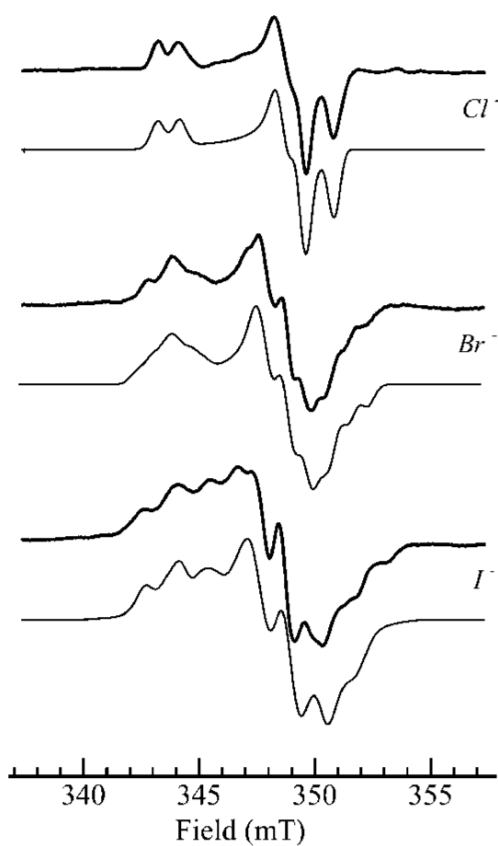


Figure 5. Comparison of the effects of chloride (0.1 M), bromide (0.2 M), and iodide (0.2 M) upon the Mo^{V} EPR spectra of human sulfite oxidase reduced with 1 mM sulfite (0.2 M bis-tris-propane, pH 6.0). The bold lines show experimental spectra and the lighter lines computer simulations using the parameters given in Table 1.

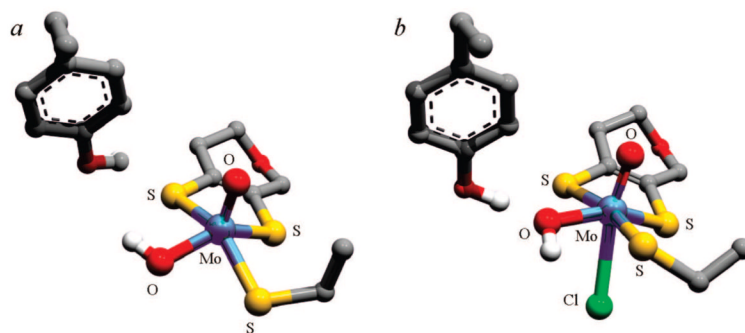


Figure 6. Postulated structures for the high-pH (a) and low-pH Cl⁻ (b) Mo^V species. Energy-minimized density functional theory structures are shown, with external atoms approximated by hydrogens (not shown).

Table 1

Mo^V Electron Paramagnetic Resonance Spin Hamiltonian Parameters^a

| | g | | | A (1H) | | | A (³⁵Cl, ⁷⁹Br, ¹²⁷I) | | | | | |
|-------------------|----------|----------|----------|---------------|----------|----------|--|----------|----------|-----------|-----------|-----------|
| | x | y | z | x | y | z | x | y | z | x' | y' | z' |
| halide-free | 1.9646 | 1.9723 | 2.0023 | 34.4 | 21.3 | 23.1 | | | | | | |
| Cl ^c | 1.9658 | 1.9724 | 2.0031 | 35.6 | 22.5 | 26.2 | 4.0 | 4.2 | | | | 4.9 |
| Br ^{c,b} | 1.9655 | 1.9732 | 2.0025 | 42 | 29 | 28 | 10 | 12 | | | | 26 |
| I ^c | 1.9670 | 1.9730 | 2.0010 | 38 | 35 | 38 | 21 | 16 | | | | 18 |

^a Values for couplings are given in MHz. As discussed in the text, the parameters for ⁷⁹Br and ¹²⁷I are difficult to unambiguously determine without measurements at a high frequency (35 GHz), because of the large number of spin Hamiltonian parameters, and these values are considered approximate. For “no halide” and Cl^c, *g* values are considered accurate to 2 on the last significant digit, and estimates of **A** to about 0.5 MHz, as discussed in the text; spin Hamiltonian parameters for the Br^c and I^c species are considered more approximate because of the number of variables in the simulations.

^b **A**(⁷⁹Br) and **g** were noncolinear ($\alpha, \beta, \gamma = 10, 57, -5^\circ$). Effects of ⁸¹Br were automatically calculated from the ratio of nuclear *g* values and nuclear electric quadrupole moments using the known natural isotopic abundance. Bromine nuclear electric quadrupole couplings were included and specified by $\mathbf{P}(x', y', z') = -2.5, +2.9, \text{ and } -0.3$ MHz with the **P** tensor held collinear with **A**.

^c **A**(¹²⁷I) and **g** were noncolinear ($\alpha, \beta, \gamma = 30, 30, -20^\circ$). Iodine nuclear electric quadrupole coupling is included and specified by $\mathbf{P}(x', y', z') = +4.3, -5.7, \text{ and } 1.3$ MHz with the **P** tensor held collinear with **A**.